

# Food & Function

Linking the chemistry and physics of food with health and nutrition

Accepted Manuscript

This article can be cited before page numbers have been issued, to do this please use: Y. Wang, F. Chen, Y. Zhang, X. Zheng, S. Liu, M. Tang, Z. Wang, P. Wang, Y. Bao and D. Li, *Food Funct.*, 2022, DOI: 10.1039/D1FO04112F.



This is an Accepted Manuscript, which has been through the Royal Society of Chemistry peer review process and has been accepted for publication.

Accepted Manuscripts are published online shortly after acceptance, before technical editing, formatting and proof reading. Using this free service, authors can make their results available to the community, in citable form, before we publish the edited article. We will replace this Accepted Manuscript with the edited and formatted Advance Article as soon as it is available.

You can find more information about Accepted Manuscripts in the [Information for Authors](#).

Please note that technical editing may introduce minor changes to the text and/or graphics, which may alter content. The journal's standard [Terms & Conditions](#) and the [Ethical guidelines](#) still apply. In no event shall the Royal Society of Chemistry be held responsible for any errors or omissions in this Accepted Manuscript or any consequences arising from the use of any information it contains.



1 **Biphasic effect of sulforaphane on angiogenesis in hypoxia via modulation of**  
2 **both Nrf2 and mitochondrial dynamics**

3 Yaqian Wang<sup>1,2,3,†</sup> · Fangfang Chen<sup>1,2,3,†</sup> · Yuan Zhang<sup>4,†</sup> · Xiangyu Zheng<sup>1,2,3</sup> · Shiyan

4 Liu<sup>1,2,3</sup> · Meijuan Tang<sup>1,2,3</sup> · Ziling Wang<sup>1,2,3</sup> · Pan Wang<sup>1,2,3</sup> · Yongping Bao<sup>5,\*</sup> · Dan Li<sup>1,2,3,\*</sup>

5 <sup>1</sup> Department of Nutrition, School of Public Health, Sun Yat-Sen University, Guangzhou, Guangdong  
6 Province 510080, P.R. China.

7 <sup>2</sup> Guangdong Provincial Key Laboratory of Food, Nutrition and Health, Guangzhou, Guangdong  
8 Province 510080, P.R. China.

9 <sup>3</sup> Guangdong Engineering Technology Center of Nutrition Transformation, Guangzhou, Guangdong  
10 Province 510080, P.R. China.

11 <sup>4</sup> Department of Geriatrics, the Third Affiliated Hospital of Guangzhou Medical University,  
12 Guangzhou, Guangdong Province 510150, P.R. China.

13 <sup>5</sup> Norwich Medical School, University of East Anglia, Norwich, Norfolk NR4 7UQ, U.K.

14 † Y. Wang, F. Chen and Y. Zhang contributed equally to this work.

15 \* Corresponding author.

16

17 **Correspondence**

18 Correspondence to Dan Li, Department of Nutrition, School of Public Health, Sun Yat-Sen University  
19 (Northern Campus), Guangzhou, Guangdong Province 510080, P.R. China. E-mail:

20 lidan58@mail.sysu.edu.cn. Or to Yongping Bao, Norwich Medical School, University of East Anglia,  
21 Norwich, Norfolk NR4 7UQ, U.K. E-mail: Y.Bao@uea.ac.uk.

22 **ORCID iD**

23 Dan Li: 0000-0001-6458-6096; Yongping Bao: 0000-0002-6425-0370

24

25 **Abstract:** Sulforaphane (SFN) is an isothiocyanate (ITC) derived from a glucosinolate, glucoraphanin  
26 found in cruciferous vegetables. There are few studies that focus on the role of SFN in angiogenesis  
27 under hypoxic conditions. The effect of SFN on angiogenesis and the underlying mechanisms  
28 including the roles of Nrf2 and mitochondrial dynamics were investigated using cultured human  
29 umbilical vein endothelial cells (HUVECs) in hypoxia. SFN at low doses (1.25-5 $\mu$ M) increased  
30 hypoxia-induced HUVEC migration and tube formation, and alleviated hypoxia-induced retarded  
31 proliferation, but high doses ( $\geq 10\mu$ M) exhibited an opposite effect. Under hypoxia, the expression of  
32 Nrf2 and heme oxygenase-1 was up-regulated by SFN treatment. Nrf2 knockdown abrogated SFN  
33 (2.5 $\mu$ M)-induced tube formation and further potentiated the inhibitory effect of SFN (10 $\mu$ M) on  
34 angiogenesis. Meanwhile, the mitochondrial function, morphology and expression of dynamic-related  
35 proteins suggested that low dose SFN protected against hypoxia-induced mitochondrial injury and  
36 alleviated hypoxia-induced fission Nrf2-dependently without affecting the expression of key effector  
37 proteins (Drp1, Fis1, Mfn1/2 and Opa1), while high concentrations ( $\geq 10\mu$ M SFN) aggravated hypoxia-  
38 induced mitochondrial injury, fission and Drp1 expression, and inhibited Mfn1/2 expression. These  
39 findings suggest that SFN biphasically affected the angiogenic capacity of hypoxia challenged  
40 HUVECs potentially via mechanisms involving an integrated modulation of Nrf2 and mitochondrial  
41 dynamics.

42  
43  
44 **Keywords:** Sulforaphane · Isothiocyanates · Angiogenesis · Hypoxia · Nrf2 · Mitochondrial  
45 dynamics

46

## 47 Introduction

48 The term “angiogenesis” is commonly used to reference the process of vessel growth but in its strictest  
49 sense it denotes vessels sprouting from pre-existing ones, and is a complex multistage process mainly  
50 involving extracellular matrix (ECM) degradation, proliferation, survival, migration, and  
51 morphological changes of endothelial cells (ECs) and their anastomosis to assemble into a vascular  
52 structure, as well as pericyte attachment. In physiological conditions, angiogenesis influences growth,  
53 development, tissue repair and menstrual cycle, but its disturbance can underlie many serious diseases,  
54 called angiogenesis-dependent diseases. Examples include: insufficient vessel growth or maintenance  
55 leading to stroke, myocardial infarction and neurodegeneration, abnormal vessel growth or remodeling  
56 contributing to pulmonary hypertension, inflammatory diseases, atherosclerosis and to most cancers.  
57 Historically, this has led to concepts of pro- and anti-angiogenic therapy, aiming to restore adequate  
58 vessel densities.<sup>1,2</sup>

59 Ischemic diseases, including myocardial infarction, stroke and peripheral vascular disease, have a high  
60 prevalence around the world and give rise to a high disability rate and mortality. Angiogenesis is both  
61 an essential adaptive response to physiological stress and an endogenous repair mechanism after  
62 ischemic injury. However, aging, diabetes, hypercholesterolemia and hypertension, the risk factors for  
63 ischemic diseases, can also constitute a deleterious macroenvironment that participate in the  
64 impairment or abrogation of post-ischemic revascularization and tissue regeneration. In turn, impaired  
65 angiogenesis can further lead to exacerbation of these diseases.<sup>3,4</sup> Identifying and using nutraceuticals  
66 and herbal medicines have become a potential therapeutic option to maintain an adequate  
67 vascularization and correct endothelial cell function or to blunt aberrant angiogenesis.<sup>5</sup>

68 Sulforaphane (4-methylsulfinylbutyl isothiocyanate, SFN) is a bioactive isothiocyanate (ITC) derived  
69 from cruciferous vegetables such as broccoli, cauliflower, cabbage and kale. It has been intensively  
70 investigated *in vitro*, in a range of animal models, and clinical trials in diseases such as cancer,  
71 metabolic diseases and neurodegenerative diseases. The beneficial effects and the lack of serious side  
72 effects observed to date, together with high bioavailability make SFN a promising candidate in the  
73 adjuvant therapy of these diseases. Underlying the remarkable efficacy are its pleiotropic activities, for  
74 example, inducing antioxidant/detoxifying enzymes, anti-inflammation, mitostatic and pro-apoptotic

75 effects, epigenetic regulation of genes, improving metabolism.<sup>6-9</sup> There is also evidence indicating that  
76 SFN and its metabolites and analogues possess anti-angiogenic properties,<sup>7,10</sup> and the potential  
77 mechanisms, though not fully elucidated, may involve inducing ECs apoptosis,<sup>11,12</sup> inhibiting matrix  
78 metalloproteinase-2/9 (MMP-2/9),<sup>13,14</sup> hypoxia-inducible factor-1 $\alpha$  (HIF-1 $\alpha$ ),<sup>13,15,16</sup> vascular endothelial  
79 growth factor (VEGF),<sup>13,15,17,18</sup> VEGF receptor-2 (VEGFR-2),<sup>13,18</sup> disrupting endothelial mitotic  
80 progression and microtubule polymerization,<sup>19</sup> anti-inflammation,<sup>20</sup> activating FOXO,<sup>21</sup> inhibiting  
81 STAT3<sup>22,23</sup> and inducing ROS.<sup>24</sup>

82 As a hormetic molecule, SFN displays characteristic biphasic dose response with a stimulatory or  
83 beneficial effect at low doses and an inhibitory or toxic effect at higher doses.<sup>25,26</sup> The hormetic  
84 property of SFN underlies many of its diverse biological activities and offers a reasonable explanation  
85 for its paradoxical effects. In regard to this, nuclear factor E2-related factor 2 (Nrf2) is an important  
86 factor.<sup>27</sup> Nrf2 is the master regulator of hundreds of transcripts, controlling cellular homeostasis  
87 through different and interconnecting effects. It can be induced by a variety of substances and stimuli,  
88 and in particular, SFN is recognized as the most classical and potent activator.<sup>10,27</sup> Evidence suggests  
89 that intracellular conjugation with GSH promotes SFN cellular uptake and concentration, and  
90 subsequently, moderate and transient cellular GSH pool depletion can adaptively induce the  
91 expressions of a battery of antioxidant/detoxifying enzymes via activation of Nrf2, providing powerful  
92 and prolonged protection against various stresses. Nevertheless, once above a concentration threshold,  
93 SFN may display cytotoxicity deriving from complex, concurring, and multiple mechanisms.<sup>25</sup>  
94 Interestingly, Nrf2 has also been confirmed to mediate pro-angiogenesis which has been documented to  
95 not only exert protective effects on several ischemic diseases but also contribute to the tumor growth,  
96 metastasis and chemo-resistant.<sup>28-31</sup>

97 Mitochondria have emerged as signaling hubs that modulate a wide range of endothelial functions  
98 including angiogenesis by coordinating reactive oxygen species, metabolism, apoptosis and calcium  
99 signaling.<sup>32</sup> Moreover, mitochondrial dynamics is also identified as a crucial determinant of  
100 angiogenesis,<sup>33</sup> which is regulated by opposing fusion and fission events via a complex protein  
101 machinery with mitofusin 1/2 (Mfn1/2) and optic atrophy (Opa1) as key pro-fusion proteins, and  
102 dynamin-related protein 1 (Drp1) and its receptors/adaptors like fission protein 1 (Fis1) as pivotal pro-  
103 fission proteins. Mitochondrial dysfunction and dynamics disorder that can result from a wide variety

104 of factors such as aging, obesity, diseases, deprivation of mitochondrial fuel substrates or oversupply of  
105 nutrients including glucose and fatty acids, hypoxia-reoxygenation/ischemia-reperfusion,  
106 hemodynamic forces, environmental and chemical stressors, contribute to the pathogenesis of complex  
107 diseases including cardiovascular disease, cancer, neurodegenerative diseases and metabolic  
108 syndrome.<sup>34-36</sup> Therefore, improving mitochondrial function and preserving mitochondrial fusion have  
109 been considered as a potent defense against compromised angiogenesis and ischemic diseases,<sup>37-39</sup>  
110 whereas inducing mitochondrial dysfunction and fission can be taken as a potential strategy for anti-  
111 angiogenic and anti-proliferative cancer management.<sup>40-42</sup> Just like the paradoxical effect on redox,  
112 modulation of mitochondrial functions by SFN is also a contradictory dual role.<sup>7,43</sup> As for  
113 mitochondrial dynamics, the investigations regarding the effect of SFN and its analogues on it and its  
114 related proteins are limited and discrepant.<sup>44-49</sup>

115 Hypoxia represents a typical characteristic of ischemia, and it is also a well-known background under  
116 which angiogenesis, no matter whether physiologically or pathologically derived, can adaptively take  
117 place. However, to date, there have been few studies investigating the effect of SFN and its analogues  
118 on angiogenesis under hypoxic conditions. Moreover, previous related research usually applies either  
119 *in vitro* culture of cancer cells or xenograft tumor models under high levels of SFN treatments,<sup>7,9</sup>  
120 because anti-angiogenesis and pro-apoptosis are the main focus of these studies. Additionally, the  
121 alteration of mitochondrial dynamics in ECs following SFN treatments and its potential role in  
122 angiogenesis have not been addressed. In the present study, we used *in vitro* primary HUVECs as a  
123 model to investigate the role of SFN in angiogenesis at a wide range of concentrations under a hypoxic  
124 condition, and to explore the potential mechanisms of Nrf2 and the mitochondrial dynamics involved.

125

## 126 **Materials and methods**

### 127 **Reagents and antibodies**

128 R, S-sulforaphane was purchased from LKT Laboratories (Minnesota, USA), with the purity  $\geq 99\%$ .  
129 WST-1 Cell Proliferation Reagent was purchased from Roche (Shanghai, China). Matrigel was  
130 purchased from BD Pharmingen (State of New Jersey, USA). Crystal violet was purchased from  
131 Beyotime Technology (Shanghai, China), JC-1 was purchased from Enzo Life Sciences, Inc (New

132 York, USA). Anti-Nrf2, anti-HO-1, anti-Mfn2, anti-Opa1, anti-Fis1, anti-Drp1, anti- $\beta$ -actin and anti-  
133 mouse IgG were purchased from Santa Cruz Biotechnology (Dallas, USA), anti-Mfn1, goat anti-rabbit  
134 IgG H&L (HRP) were purchased from Abcam (Cambridge, UK).

#### 135 **Cell culture and hypoxic exposure**

136 HUVECs were obtained from ScienCell Research Labs and cultured in Endothelial Cell Medium  
137 (ECM) containing 5% fetal bovine serum (FBS), 1% endothelial cell growth supplement (ECGS) and  
138 1% penicillin/streptomycin (P/S) (ScienCell, San Diego, CA) at 37°C in a humidified atmosphere  
139 containing 5% CO<sub>2</sub>. Cells between passages 2 and 8 were used for all experiments. For hypoxia  
140 exposure, cells were subjected to hypoxia in a sealed incubator container (Unitech, Guangzhou, China)  
141 that was flushed with a gas mixture of 1% O<sub>2</sub>, 5% CO<sub>2</sub>, and balance N<sub>2</sub> by using Anoxomat MarkIII  
142 (Advanced instruments Inc., California, Pomona, USA). The container was then placed in a humidified  
143 37°C incubator.

#### 144 **Cell proliferation assay**

145 HUVECs proliferation was determined by a WST-1 cell proliferation assay. Cells were seeded in 96-  
146 well culture plates at a density of  $1 \times 10^4$  per well and cultured in complete medium overnight, and then  
147 exposed to increasing concentrations of SFN (1.25, 2.5, 5, 10, 20, 40, 80 or 100  $\mu$ M) for 24h under  
148 hypoxic conditions. The control groups were treated with a DMSO concentration equal to the highest  
149 percentage (1%) under a hypoxic or normoxic condition. After treatment, 10  $\mu$ L WST-1 solution was  
150 added to each well, and the plates were incubated for an additional 4 h at 37°C, then shaken thoroughly  
151 for 1min on a shaker. Optical density was measured using a microplate reader (Bio-Tek instrument Inc,  
152 Vermont, USA) at a test wavelength of 440nm and a reference wavelength of 620nm. The IC<sub>50</sub> was  
153 determined using CalcuSyn software version 2.0 (Biosoft, Cambridge, UK).

#### 154 ***In vitro* migration assay**

155 Cell migration assays were performed using 24-well modified Boyden chambers (Corning Life  
156 Science, Corning, NY, USA) containing a polycarbonate filter with a pore size of 8- $\mu$ m, according to  
157 the manufacturer's protocol. HUVECs were added to the upper chamber of the insert in 200  $\mu$ L of  
158 serum-free medium. Medium (600  $\mu$ L) with 5% FBS was added to the lower chamber. To determine



159 the effect of SFN on cell migration, different concentrations of SFN were added to the lower chamber,  
160 then the transwell chambers were incubated for 24h under hypoxic conditions at 37°C (DMSO  
161 treatments in hypoxia and normoxia were used as controls). After the incubation period, the non-  
162 migrated cells on the upper chambers were removed with cotton swabs. The cells that had migrated  
163 through the pores of the membrane to the bottom chambers were fixed with 4% paraformaldehyde for  
164 15 min and then stained with 0.1% crystal violet for 15 min. Cell migration was quantified by counting  
165 the number of cells from five random fields for each membrane using an inverted fluorescence  
166 microscope (Nikon, Tokyo, Japan) at 100× magnification.

### 167 **Capillary-like structure formation assay**

168 Matrigel (70  $\mu$ L/well) was added to a 96-well plate and incubated at 37°C for 1 h. HUVECs ( $3 \times 10^4$   
169 cells) were seeded onto each well of the Matrigel-coated 96-well plate and then incubated in complete  
170 culture medium with various concentrations of SFN in hypoxia with DMSO (<1‰) treatments in  
171 hypoxia and normoxia used as controls. After incubation for 8 h, the formation of the endothelial cell  
172 tubular structures was visualized under an inverted microscope (Carl Zeiss AG, Aalen, Germany) and  
173 photographed at 100× and 200× magnification. Five randomly chosen fields for each well were  
174 photographed and analyzed with an image analysis system (ImageInside Ver 3.32) for the quantitation  
175 of the number of meshes and master junctions as well as the total length of branches.

### 176 **Electron microscopy**

177 HUVECs were fixed in 2.5% glutaraldehyde at 4 °C for 2h, then rinsed with 0.1 M phosphate buffer 6  
178 times for 15 minutes each. After fixation in 1% osmic acid for 1.5h, the cells were subjected to gradient  
179 alcohol dehydration and resin penetration, then embedded in Epon812 pure resin. Ultrathin sections (50  
180 nm) were generated by Ultrathin Microtome (Leica, Weztlar, Germany), then transferred to copper  
181 grids, and analysed by transmission electron microscopy (Japan Electron Optics Laboratory Co., Ltd.,  
182 JEM-1400 PLUS). Images were taken at 30,000×magnification.

### 183 **Measurement of mitochondrial membrane potential**

184 Mitochondrial membrane potential ( $mt\Delta\Psi$ ) was detected by using a fluorescence probe JC-1 according  
185 to the manufacturer's instructions. In brief, HUVECs following different treatments for 24h were

186 incubated with 5  $\mu\text{g}/\text{mL}$  JC-1 at RT for 15 min, and then washed twice with PBS. The fluorescence of  
187 JC-1 was immediately detected at wavelengths of 530 nm (green) and 590 nm (red) by a microplate  
188 reader (Bio-Tek instrument Inc, Vermont, USA). The value of  $\text{mt}\Delta\Psi$  was calculated as the ratio of red  
189 fluorescence intensity to green fluorescence intensity.

### 190 **Mitochondrial morphology**

191 To assess mitochondrial fusion and fission, mitochondria were stained and photographed. In brief,  
192  $2 \times 10^5$  cells were plated on 35 mm glass bottom microwell dishes (Mat-Tek, Ashland, MA) and  
193 cultured overnight, then treated with DMSO (<1%) in normoxia or hypoxia or SFN (2.5, 10  $\mu\text{M}$ ) in  
194 hypoxia for 24h. After treatment, the cells were washed twice with cold PBS and incubated with  
195 medium containing 100nM MitoTracker<sup>TM</sup> Green FM (Thermo Fisher Scientific, Carlsbad, USA) at 37  
196  $^{\circ}\text{C}$  for 30 min in the dark, then washed with PBS. Mitochondria in live cells were visualized using  
197 laser confocal scanning microscopy (TCS SP5) with a HC $\times$ PL APO CS 40 $\times$ 1.3 OIL objective (Leica,  
198 Weztlar, Germany). The images were acquired with Leica confocal software and analyzed with an  
199 image analysis system (Image Inside Ver 3.32) to determine the mitochondrial lengths and circularity.

### 200 **Cell transfection with Nrf2 siRNA**

201 For RNA interfering knockdown, subconfluent HUVECs were transfected with 10 nM Nrf2 siRNA  
202 duplex or control siRNA (Santa Cruz Biotechnology, Dallas, USA) using lipo3000 reagent (Thermo  
203 Fisher Scientific, Massachusetts, USA) for 8 h. The medium was then replaced and incubation  
204 continued for 24h under normoxia, followed by SFN (2.5, 10  $\mu\text{M}$ ) or DMSO (<1%) intervention under  
205 hypoxia for 24h. Transfection efficiency was confirmed by Western blot.

### 206 **Western blot analysis**

207 After treatment for 24h, the total protein was extracted from the whole cells following standard  
208 procedures, and concentrations were quantified by a BCA protein assay kit (Beyotime Technology,  
209 Shanghai, China). Equal amounts of protein were separated by sodium dodecyl sulfate-polyacrylamide  
210 gels electrophoresis (SDS-PAGE), and then transferred onto a polyvinylidene fluoride (PVDF)  
211 membrane (Millipore, Bedford, MA). The membranes were blocked with 5% skimmed milk in TBST  
212 (0.1% Tween 20) at RT for 1.5 h, and then incubated with a specific primary antibody overnight at 4 $^{\circ}\text{C}$

213 at a dilution of 1:500 for Nrf2, 1:600 for HO-1, 1:1000 for Mfn1, Mfn2, Fis1, Drp1, Opa1 and  $\beta$ -actin  
214 The membranes were washed three times for 15 min with TBST, followed by incubation with  
215 secondary antibody diluted at 1:10000 for goat anti-rabbit IgG and 1:4000 for anti-mouse IgG for 1 h at  
216 RT. After further washing, protein bands were visualized with ECL reagent (Thermo Fisher, Rockford,  
217 USA) and densitometry was measured by Image J.

## 218 **Statistical analysis**

219 The data are presented as means  $\pm$  SD. Differences between groups were assessed by performing one-  
220 way ANOVA using SPSS 19.0 software (SPSS Inc, Chicago, IL, USA).  $P < 0.05$  was considered  
221 statistically significant.

222

## 223 **Results**

### 224 **Biphasic effect of SFN on angiogenesis in HUVECs under hypoxia**

225 ECs proliferation, migration and tube formation are the key steps of angiogenesis.<sup>1,2</sup> Therefore, the  
226 effect of a range of concentrations of SFN treatment (1.25-100  $\mu$ M for 24 h) on proliferation of  
227 HUVECs was measured by a WST-1 assay under hypoxia. As presented in **Figure 1a**, hypoxia  
228 treatment alone suppressed HUVECs proliferative activities by 20.7% compared to normoxia control.  
229 Under hypoxic conditions, SFN treatment exerted a biphasic effect on HUVECs proliferative capacity.  
230 Low doses (1.25-5  $\mu$ M) of SFN had no cytotoxicity, but instead promoted cell proliferation to 127.0-  
231 146.8% of hypoxia control with the maximal induction occurring at 2.5  $\mu$ M. In comparison to hypoxia  
232 control, there was no significant difference in cell viability at 24h post 10  $\mu$ M SFN exposure, however,  
233 once beyond this concentration threshold, a dose-dependent inhibitory effect was observed. These  
234 inhibition rates dramatically rose from 36.8 to 94.1% with increasing concentrations with the  $IC_{50}$  of  
235 about 27.6  $\mu$ M. Thus, to avoid severe cytotoxicity, a concentration range of 1.25-20  $\mu$ M was used for  
236 the subsequent evaluation assays and the mechanistic studies.

237 The effect of SFN on HUVECs migration under hypoxia was then explored using transwell assays. The  
238 results showed that there was a small increase (about 22.2%) in the number of HUVECs migrating to  
239 the lower side of the filter through the transwell membrane (8  $\mu$ m pore size) after hypoxia exposure,

240 which was further potentiated by 2.5  $\mu$ M SFN co-exposure (an additional 35.8% increase or 129.3% of  
241 hypoxia control) despite no significant alteration at 1.25 and 5  $\mu$ M SFN co-exposures. However, 10,  
242 20  $\mu$ M SFN inhibited cell migration under hypoxia in a dose dependent manner (68.6% and 53.4% of  
243 hypoxic control, respectively) (**Fig. 1b, c**).

244 The matrigel assay was performed to determine capillary-like structure formation capacity in the  
245 model, which was quantified as the number of tube-like structures (meshes) and nodes and also as the  
246 total branching length of tube networks. Similarly, as depicted in **Figure 1d-g**, the biphasic regulatory  
247 effect was also found to be exerted by SFN on capillary-like structure formation in HUVECs under  
248 hypoxia. A significant increase in the ability of HUVECs to form tube-like structures was detected  
249 after 24h hypoxia treatment (140.2, 130.7, and 121.5% increase in the number of meshes, nodes and the  
250 total branching length, respectively), which was further substantially enhanced by lower doses ( $<5 \mu$ M)  
251 of SFN but markedly disrupted by higher doses ( $\geq 10 \mu$ M) with no completely formed networks in 20  
252  $\mu$ M SFN treatment group. Compared to hypoxia control, the number of meshes and nodes was  
253 increased by 46.0 to 92.4% and 21.3 to 56.7%, respectively, at 1.25-2.5  $\mu$ M SFN, whereas decreased  
254 by 25.6 to 98.7% and 17.8 to 89.9%, under 10-20  $\mu$ M SFN treatments; the total length of tube networks  
255 was increased by 15.7% at 2.5  $\mu$ M SFN, whereas decreased by 11.6 to 83.4% at 10-20  $\mu$ M SFN.

256 Collectively, these data suggest that SFN administration can display a dose-dependent biphasic effect  
257 on hypoxia-induced angiogenesis *in vitro* HUVECs, reinforcing it at lower concentrations ( $<5 \mu$ M)  
258 whereas inhibiting it at higher concentrations ( $\geq 10 \mu$ M).

259

### 260 **Nrf2/HO-1-mediated pro-angiogenesis contributes to the angio-modulatory property of SFN in** 261 **HUVECs under hypoxia**

262 Nrf2 and its down-stream target gene HO-1, the pivotal mediators of multiple biological activities of  
263 SFN,<sup>10,27</sup> are also implicated in pro-angiogenesis.<sup>28-31</sup> Therefore the degree to which they interfere in  
264 the regulation of angiogenesis by SFN under hypoxia was investigated. HUVECs were exposed to  
265 either normoxia or hypoxia treatment or SFN treatment under hypoxia conditions for 24h, and then the  
266 protein levels of Nrf2 and HO-1 in the whole cells were detected by immunoblotting analysis. As

267 expected, SFN (2.5-20 $\mu$ M) significantly up-regulated the expression of Nrf2 and HO-1 in a dose-  
268 dependent manner in hypoxia (**Fig. 2a, b**). Hypoxia treatment alone also led to a slight increase in Nrf2  
269 expression as compared to normoxia, but the difference was not statistically significant.

270 In addition, the angiogenic capacity of HUVECs following SFN treatment under hypoxia was  
271 evaluated following knockdown of Nrf2. HUVECs were transfected with Nrf2 siRNA or scrambled  
272 siRNA for 8h, the medium was then replaced and incubation continued for 24h under normoxia,  
273 followed by 2.5 or 10  $\mu$ M SFN treatment in hypoxia for a further 24h with DMSO (<1%) as a solvent  
274 control. Compared with the scrambled control, transfection with Nrf2 siRNA significantly abated the  
275 protein expressions of Nrf2 and HO-1, indicating that knockdown of Nrf2 by siRNA transfection was  
276 effective in HUVECs (**Fig. 2c, d**). Next, as shown in **Fig. 2e-h**, knockdown of Nrf2 not only reduced  
277 the constitutive angiogenesis in hypoxia, but also inhibited angiogenesis following 2.5 $\mu$ M SFN  
278 treatment, and even exacerbated 10 $\mu$ M SFN-induced anti-angiogenesis. These results reveal that  
279 Nrf2/HO-1 mediated pro-angiogenesis contributes to the angio-modulatory property of SFN under  
280 hypoxia.

281

### 282 **SFN treatment bilaterally affects hypoxia-induced mitochondrial injury and fission in HUVECs**

283 Mitochondria are essential cellular organelles and are key players in a plethora of physiological and  
284 biochemical processes.<sup>36</sup> Accordingly, it is of great significance to analyze the change in their  
285 structures, forms and functions following hypoxia exposure and SFN co-exposure. Firstly,  
286 mitochondrial ultrastructures were examined by transmission electron microscopy (TEM). TEM  
287 images confirmed that hypoxia caused mitochondrial damage, including cristae disappearance,  
288 mitochondrial swelling, mitochondrial vacuolation, matrix dissolution, and mitochondrial pyknosis,  
289 which were relieved by 2.5 $\mu$ M SFN treatment but aggravated by a SFN treatment concentration of  
290 10 $\mu$ M (**Fig. 3a**). For quantification, at least 300 mitochondria per condition were analyzed.  
291 Mitochondrial injuries were categorized into entirely damaged and partially damaged phenotypes, and  
292 the former was scored in the absence of cristae and the latter scored if some cristae were present,  
293 compared to intact mitochondria with normal cristae. The structural data verified the mitoprotection by  
294 the lower dose of SFN and the worsening effect by the higher dose in response to hypoxia-triggered

295 mitochondrial injury (**Fig. 3b**).

296 Mitochondrial membrane potential ( $mt\Delta\Psi_m$ ) is a universal indicator of mitochondrial health and the  
297 loss of it indicates mitochondrial dysfunction or injury. The change of  $mt\Delta\Psi_m$  during hypoxia and the  
298 influence of SFN administration were assessed using a voltage-sensitive JC-1 fluorescence probe and  
299 spectrofluorometry, and  $mt\Delta\Psi_m$  values were calculated as the ratio of red to green fluorescence  
300 (aggregate/monomer). Consistent with the mitochondrial ultrastructure by TEM, quantitative analysis  
301 data (**Fig. 3c**) showed that there was significant loss (about 43.0%) of  $mt\Delta\Psi_m$  in HUVECs subjected to  
302 hypoxia for 24h as compared to those in normoxia. SFN treatment displayed a dose-dependent opposite  
303 role in hypoxia-evoked  $mt\Delta\Psi_m$  reduction. SFN treatments from 1.25 and 2.5 $\mu$ M tended to block the  
304 decrease in  $mt\Delta\Psi_m$  induced by hypoxia with a statistically significant difference ( $\times 1.7$  fold) from  
305 hypoxia control at 2.5 $\mu$ M. Conversely, 10 and 20 $\mu$ M SFN treatments further dose-dependently  
306 enhanced hypoxia-caused depolarization of mitochondria (36.3-46.3% of hypoxia control).

307 Mitochondria, as highly dynamic and sensitive organelles, constantly regulate the balance between  
308 fusion and fission in response to various stimuli.<sup>35</sup> Moreover, mitochondrial dynamics is not only a  
309 crucial determinant of angiogenesis,<sup>33</sup> but also emerges as a potential target of SFN and its  
310 analogues.<sup>44-49</sup> To examine the change of balance of mitochondrial dynamics in HUVECs following  
311 hypoxia treatment and the influence of SFN treatment, MitoTracker Green dye was used to visualize  
312 mitochondrial morphology by confocal microscopy and computer-assisted morphometric analysis was  
313 performed to measure mitochondrial lengths and circularity with higher values indicating more  
314 rounded mitochondria and a perfect circle equal to 1.0. As depicted in **Figure 3d-f**, mitochondrial  
315 morphology in the hypoxia-treated group differed from that in the normoxia group, and this was  
316 manifested as multiple, round, discriminative puncta and fewer networks which was quantified as a  
317 shorter average length and a higher circularity value. However, the abnormal mitochondrial  
318 morphology in HUVECs exposed to hypoxia was improved when co-exposed to 2.5 $\mu$ M SFN since the  
319 latter preserved a more elongated phenotype. Conversely, compared to hypoxia control, there was mild  
320 reduction in mitochondrial lengths and augmentation in circularity when exposed to 10 $\mu$ M SFN.

321 Taken together, these data suggest that hypoxia exposure results in mitochondrial injury and  
322 imbalances mitochondrial dynamics toward increased fission, and these disturbances are

323 bilaterally affected by SFN co-exposure with a protective effect at low doses but a deteriorative effect  
324 at high doses.

325

326 **Inducing Drp1 and suppressing Mfn1/2 expression by SFN at high doses correlate with its**  
327 **promotion of hypoxia-induced fission in HUVECs**

328 Mitochondrial dynamics is manipulated by the balance between fission, and fusion related proteins. To  
329 understand mechanistically the changes of mitochondrial morphology in different intervention  
330 conditions, the levels of five key mitochondrial dynamic regulatory proteins were determined,  
331 including pro-fissioned Drp1 and its adaptor Fis1 as well as pro-fused Mfn1/2 and Opa1.

332 Representative blots and the average relative protein expressions are presented in **Figure 4**. Hypoxia  
333 significantly increased Drp1 levels, but had no effect on other proteins. Low concentrations (1.25-5 $\mu$ M)  
334 of SFN treatments did not affect any dynamics related protein expressions under hypoxia, while higher  
335 concentrations (10 and 20 $\mu$ M) treatments induced a further and remarkable dose-dependent increase in  
336 Drp1 expression in parallel with significant decreases in Mfn1/2. No significant changes were  
337 identified in Fis1 and Opa1 levels after high doses SFN treatments. These results, in combination with  
338 the above morphological changes of mitochondria, infer that high doses of SFN aggravate hypoxia-  
339 induced fission through a mechanism involving induction of Drp1 protein and inhibition of Mfn1/2  
340 proteins. Low doses of SFN induced defense against hypoxia-caused fission may be dependent on  
341 regulating the detected dynamics related proteins activities via post-translational modification and/or  
342 implicate other undetected mitochondrial dynamics related proteins.

343

344 **Effect of SFN on mitochondrial morphology after Nrf2 knockdown in HUVECs under hypoxia**

345 Given the core role of Nrf2 in appropriate concentrations of SFN induced antioxidant defense<sup>10</sup> and the  
346 significance of redox modulation of fusion and/or fission proteins activities,<sup>50,51</sup> it can be speculated  
347 that the mechanism of alleviating hypoxia-induced fission by SFN at low doses is probably due to the  
348 modulation of mitochondrial dynamics related protein activities via Nrf2-dependent  
349 redox modification. This possibility was preliminarily explored by evaluating the mitochondrial

350 morphology change elicited by SFN in hypoxia again after Nrf2 knockdown. HUVECs were  
351 transfected with Nrf2 siRNA or scrambled siRNA for 8h, the medium was then replaced and  
352 incubation continued for 24h under normoxia, followed by 2.5 or 10  $\mu$ M SFN treatment in hypoxia for  
353 an additional 24h with DMSO (<1%) as a solvent control. Subsequently, mitochondrial morphology  
354 was detected by MitoTracker Green staining. The results showed that, compared to the equivalent  
355 siCont group, the circularity values in both 2.5 and 10 $\mu$ M SFN-treated as well as DMSO-treated siNrf2  
356 cells were all significantly elevated while the average mitochondrial lengths were all significantly  
357 diminished (**Fig. 5**). This is indicative of the importance of Nrf2 in both basal and low levels of SFN-  
358 induced defense against mitochondrial fission under hypoxia, as well as the contribution of Nrf2 to  
359 counteract to mitochondrial dynamic imbalance when concurrently suffering from high levels of SFN  
360 and hypoxia exposures.

361

## 362 Discussion

363 Like several other extensively studied dietary phytochemicals,<sup>52</sup> SFN has been documented to be a  
364 hormetic agent.<sup>25,26</sup> Low doses of these compounds may prepare cells to resist more severe stress by  
365 activating signaling pathways that result in increased expression of genes encoding cytoprotective  
366 proteins, but in contrast, high doses are cytotoxic. Some studies have also discovered that high doses of  
367 SFN and its analogues can have anti-angiogenic activities, however, few researchers have paid  
368 attention to what happens with treatments at low doses. Only two studies have been carried out on the  
369 direct effect of ITCs on angiogenesis under hypoxic conditions, showing an inhibitory effect on colon  
370 and glioma cancer cell migration.<sup>15,16</sup> In the present study, by using *in vitro* primary HUVECs as a  
371 model, we demonstrate for the first time that SFN displays a biphasic effect on angiogenesis in hypoxia  
372 and that the potential mechanisms involve an integrated modulation of Nrf2 and mitochondrial  
373 dynamics.

374 Hypoxia/Ischemia may result in EC injuries particularly manifested as mitochondrial dysfunction,<sup>53</sup>  
375 however, they can also adaptively trigger angiogenesis.<sup>3</sup> Both physiological and pathological  
376 angiogenesis can occur in a hypoxia/ischemia context, so *in vitro* hypoxia was adopted here to mimic  
377 the *in vivo* context to explore the effect of SFN on angiogenesis. The results showed that hypoxia



378 promoted the migration and tube-like structure formation by HUVECs despite inhibiting their  
379 proliferation to a certain extent (**Fig. 1**). A similar finding was reported by Befani and Liakos in human  
380 microvascular endothelial cells (HMECs).<sup>54</sup> Hypoxia-induced migration and/or tube formation have  
381 also been observed in HUVECs,<sup>55</sup> human endothelial cell line EA.hy 926,<sup>56</sup> human pulmonary artery  
382 endothelial cells (PAECs)<sup>57</sup> and rat aortic endothelial spheroids<sup>58</sup> models, but conversely the opposite  
383 effects have also been reported.<sup>59,60</sup> Most but not all studies have shown that hypoxic exposure can  
384 inhibit the proliferative activity of ECs,<sup>58,61,62</sup> and some data suggest that normal ECs such as HUVECs  
385 are more sensitive than ECs from tumors.<sup>63</sup> Hence it will be of great significance to detect and mimic  
386 the specific hypoxic intensities in different physiopathology conditions and tissue types in the future  
387 since the influence of hypoxia on angiogenesis can be very different depending on the degree, duration  
388 and frequency of hypoxia as well as the cell types.

389 Under the hypoxic background, we demonstrated that SFN also has a hormetic effect on the angiogenic  
390 capacity of HUVECs, characterized by potentiating hypoxia-induced angiogenesis at low doses (1.25  
391 and 2.5 $\mu$ M), but inhibiting it at high doses ( $\geq 10\mu$ M) (**Fig. 1**). Similarly, this bell-shaped effect of SFN  
392 and its analogues on angiogenesis in normoxia has also been found in our previous studies utilizing  
393 tumor cells and 3-D HUVECs and pericyte co-culture models.<sup>17,22,24,64</sup> The stimulating action of SFN  
394 on angiogenesis has been evidenced in ethanol-injected chick yolk sac membrane (YSM) and  
395 chorioallantoic membrane (CAM) models at 2.5-10 $\mu$ M co-treatment,<sup>65</sup> and in 2.5 $\mu$ M-pretreated  
396 endothelial colony forming cells (ECFCs).<sup>66</sup> In contrast, anti-angiogenic activities of SFN and some  
397 other ITCs have also been reported in HUVECs and rat aortic ring models at a single dose ( $> 10\mu$ M) of  
398 intervention in normoxia.<sup>20,21</sup> Additionally, dose-dependent inhibition of HUVECs proliferation and  
399 capillary-like tube formation in normoxia by SFN ( $\geq 10\mu$ M) has been demonstrated by Asakage *et al*  
400 and Nishikawa *et al*, but no effects were detected at intervention concentrations below 10 $\mu$ M.<sup>11,12</sup>  
401 Notably, compared to HUVECs, human microvascular ECs appeared much more sensitive to SFN-  
402 induced anti-angiogenesis since 0.3 $\mu$ M and 0.1 $\mu$ M SFN have been found capable of suppressing  
403 angiogenesis in these models.<sup>13,14</sup> Additionally, the anti-angiogenic thresholds of phenethyl  
404 isothiocyanate (PEITC) and benzyl Isothiocyanate (BITC) were found to be lower than that of SFN.<sup>18,23</sup>  
405 Given these limited reports and discrepant results, further studies are required to determine whether the  
406 biphasic effect of SFN on angiogenesis in hypoxic HUVECs can likewise exist in other hypoxic ECs

407 and tumor cells, whether other ITCs may also possess the similar angio-hormetic property, and what  
408 are the consequences *in vivo* under different physiological and pathological conditions.

409 Nrf2 is a major regulator of cellular response to diverse stresses, and mediates multiple biological  
410 effects of SFN.<sup>10,27</sup> The pro-angiogenic roles of Nrf2 and its target gene HO-1 as well as their  
411 protections on ischemic diseases and their implications in some pathogenic consequences like cancer,  
412 have all been demonstrated.<sup>28-31</sup> It has been reported that Nrf2 dysfunction may be a potential  
413 mechanism underlying impaired angiogenesis and microvascular rarefaction in aging.<sup>4</sup> Therefore,  
414 whether and how Nrf2 can interfere in the SFN-modulated angiogenesis in hypoxia was further  
415 explored. Firstly, as expected, SFN increased the levels of Nrf2 and HO-1 protein dose-dependently  
416 (**Fig. 2a, b**) and secondly, knockdown of Nrf2 and the consequent down-regulation of HO-1 protein  
417 expression not only reduced the constitutive angiogenesis in hypoxia, but also substantially inhibited  
418 the 2.5 $\mu$ M SFN-induced angiogenesis, and even exacerbated the anti-angiogenesis by 10 $\mu$ M SFN in  
419 hypoxia (**Fig. 2c-h**). Nrf2-mediated angiogenesis has been reported to play an important role in the  
420 angiogenic capacity of ECFCs, particularly under conditions of increased oxidative stress, which  
421 constitutes the likely mechanism whereby SFN (2.5  $\mu$ M) promoted basal angiogenesis and preserved  
422 ROS-inhibited angiogenesis in normoxia.<sup>66</sup> Additionally, it has been reported that silencing of Nrf2  
423 abolished 2.5 $\mu$ M allyl isothiocyanate (AITC)-stimulated HepG2 cell migration<sup>24</sup> and 2.5 $\mu$ M SFN-  
424 induced vascular-like structures formation in normoxia<sup>67</sup> as well as hypoxia-induced angiogenesis.<sup>68</sup>  
425 The findings here offer further support that the positive role of Nrf2/HO-1 also mediates the angio-  
426 modulatory property of SFN in HUVECs under hypoxia.

427 Corresponding to the angio-hormetic effect, a mito-hormetic effect of SFN on HUVECs in hypoxia  
428 was also revealed in this study. Mitochondrial ultrastructure, membrane potential and morphology  
429 analysis showed that low doses of SFN improved hypoxia-induced mitochondrial injury, dysfunction  
430 and dynamic imbalance, while high doses worsened the abnormalities (**Fig. 3**). Modifications of  
431 mitochondrial signaling, functionality, and integrity by SFN have been widely reported, however,  
432 seemingly contradictory behaviors have been discovered. SFN can exert cyto- and mito-protective  
433 effect against ROS, toxins, ischemia, hypoxia and other attacks, but conversely it can cause deleterious  
434 changes in mitochondria that would eventually carry the cell to death.<sup>43</sup> Evidence also exists to indicate  
435 that the toxicity of SFN appears to be cancer cell specific,<sup>25</sup> nevertheless, our findings in HUVECs

436 suggested that this is not always the case. Apart from cell types, the paradoxical phenomena observed  
437 in our study suggested that exposure doses and context are crucial determining factors. Notably, most  
438 studies dealing with SFN toxicity report effects occurring at concentrations above 5-10 $\mu$ M.<sup>25</sup> Some  
439 investigations have shown that induction of mitochondrial dysfunction and fission can destroy  
440 angiogenesis<sup>40-42</sup> while improvement of mitochondrial function and promotion of fusion have the  
441 opposite effect.<sup>33,37-39</sup> Consequently, we speculate that the mito-hormetic effect of SFN might also  
442 contribute to its angio-hormetic effect in HUVECs under hypoxia.

443 Mitochondrial fusion and fission are coordinated by several dynamics related proteins, principally pro-  
444 fused Mfn1/2 and Opa1 and pro-fission protein Drp1 and its adaptor Fis1. The data on the effect of  
445 SFN and its analogues on the expression of these proteins is limited and inconsistent.<sup>44-49</sup> In addition, it  
446 was reported that Nrf2 can promote mitochondrial hyper-fusion through degradation of Drp1 levels<sup>69</sup>  
447 and some of its activators may ameliorate unbalanced mitochondrial dynamics caused by different  
448 pathogenic factors<sup>70</sup>. Therefore, the expressions of these key dynamics related proteins were further  
449 examined. In agreement to the above mitochondria morphology, hypoxia led to an up-regulated Drp1  
450 expression despite no significant alteration in Mfn1/2, Opa1 and Fis1 observed. Similarly,  
451 hypoxia/ischemia induced-fission and Drp1 expression have also been reported to mediate stem cell  
452 apoptosis and tissue /cell damage.<sup>71,72</sup> Unexpectedly, SFN treatment did not improve hypoxia-induced  
453 abnormality in Drp1 expression, but conversely, 10 and 20 $\mu$ M SFN treatment potentiated the hypoxia-  
454 induced Drp1 expression and concurrently inhibited Mfn1/2 expression. Notably, in hypoxia, low doses  
455 (1.25-5 $\mu$ M) of SFN had no significant influence on any detected dynamics related protein levels,  
456 although the reversed hypoxia-induced fission was observed at 2.5 $\mu$ M SFN (**Fig. 3d-f and 4**). Hence,  
457 we infer that the phasic regulatory activity of SFN on mitochondrial dynamics in hypoxia might be  
458 ascribed to both transcriptional/translational regulation and posttranslational modification mechanism  
459 (PTM), that is improving hypoxia-induced fission via modulation of certain dynamics related proteins  
460 activities by PTM at low doses, whereas deteriorating that via up-regulation of Drp1 and down-  
461 regulation of Mfn1/2 levels as well as the non-excluded PTM.

462 Redox, phosphorylation, acetylation, and ubiquitylation are the main potential PTM in controlling  
463 certain fusion and fission proteins activities,<sup>34-36,50</sup> and most of their related signal pathways or effectors  
464 are also the targets of SFN and /or Nrf2. Given redox perturbation elicited by hypoxia, links between

465 ROS/RNS modification of certain dynamics related proteins and fission,<sup>50,51</sup> and the core role of Nrf2  
466 in antioxidant defense, it can be speculated that the mechanism of alleviating hypoxia-induced fission  
467 by SFN at low doses is likely by Nrf2-dependent redox modulation of certain dynamics related proteins  
468 activities. This possibility was preliminarily validated here by findings that Nrf2 knockdown inhibited  
469 low dose SFN-induced fusion in hypoxia. The pro-fusion role of Nrf2 was not confined to low doses of  
470 SFN treatment and also existed when exposed to higher doses of SFN and hypoxia *per se* (**Fig. 5**), a  
471 finding compatible with the above positive mediated role of Nrf2 in angiogenesis. Further precise  
472 studies are needed to determine the redox homeostasis in cells and mitochondria, as well as to elucidate  
473 which dynamics related proteins and which amino acid residues are the key redox modification targets.  
474 The possibility that Nrf2-dependent non-redox PTM also requires consideration and confirmation.

475 Modulation of mitochondrial dynamics by SFN and its analogues has become a novel and intriguing  
476 research topic. Both their cytoprotective response by inhibiting fission and pro-apoptotic effects via  
477 inhibiting fusion have been reported.<sup>40,44</sup> Even circular mitochondria formed by granular mitochondria  
478 were detected in SFN treated cancer cells.<sup>45</sup> Moreover, the mechanisms whereby SFN and its analogues  
479 affect mitochondrial dynamics are not yet well understood. Mitigating the recruitment and /or retention  
480 of the soluble Drp1 to mitochondria without changing overall Drp1 abundances was reported to  
481 mediate inhibiting fission in human retinal pigment epithelial (RPE-1) cells by 50 $\mu$ M SFN treatment  
482 for 4h,<sup>46</sup> yet reversing iron-induced Drp1 protein reduction in hippocampus has also been found  
483 associated with neuroprotection by SFN.<sup>47</sup> In contrast, BITC (2.5 and 5 $\mu$ M for 6h) induced fission  
484 accompanied by both decreases in pro-fusion and pro-fission proteins, and this effect was cancer cell  
485 specific.<sup>48</sup> Nevertheless, although treating breast cancer cells with 20 $\mu$ M erucin for 6h can also induce  
486 fission and apoptosis, the mechanism was due to inducing mitochondrial translocation of Drp1.<sup>49</sup> The  
487 results here, together with other previous findings, suggest that the discrepancy in the effect of SFN  
488 and its analogues on mitochondrial dynamics may be due to the differences in study models and  
489 context, intervention duration and timing (pre, co- and post-treatment), exposure doses, as well as ITCs  
490 types, all of which deserve further exploration.

491

## 492 **Conclusion**

493 The present study innovatively demonstrates that SFN exhibits a dose-dependent biphasic effect on  
494 angiogenesis in hypoxia challenged HUVECs via mechanisms involving an integrated modulation of  
495 Nrf2 and mitochondrial dynamics. Nrf2 activation by SFN at moderate doses (1-5 $\mu$ M, achievable in  
496 human plasma *via* dietary intake of cruciferous vegetables <sup>9</sup>) contributes to the protection against  
497 hypoxia-evoked mitochondrial injury and fission thus boosting the angiogenic capacity of HUVECs.  
498 However, under high pharmacological doses of SFN exposure, the induction of mitochondrial fission  
499 resulting from up-regulating Drp1 and down-regulating Mfn1/2, coupled with aggravated  
500 mitochondrial injury, overwhelms Nrf2-mediated defenses, hence generating an angio-inhibitory effect.  
501 Our findings enrich the knowledge of the hormetic character of SFN from the angle of angiogenesis in  
502 hypoxia. The discovery of crosstalk between mitochondrial dynamics and Nrf2 in mediating SFN  
503 action in angiogenesis, and the complex regulatory mechanism of SFN on mitochondrial dynamic infer  
504 that, mitochondrial dynamics deserves further focusing when exploring and interpreting SFN bio-  
505 efficacy. Given the limitation of cell-based *in vitro* experiments and the different consequence of  
506 angiogenesis in therapeutic/reparative angiogenesis and aberrant angiogenesis related diseases, further  
507 *in vivo* studies with exposure to a wide range of SFN concentrations under specific angiogenesis-  
508 related disease backgrounds are warranted.

509

#### 510 **Author contributions**

511 Dan Li and Yongping Bao contributed to the study design and manuscript writing. Yaqian Wang,  
512 Fangfang Chen and Yuan Zhang performed the experiments. Yaqian Wang and Xiangyu Zheng  
513 conducted data analysis. Shiyan Liu drew the graphic for proposed mechanism. Meijuan Tang, Ziling  
514 Wang and Pan Wang revised the manuscript.

515

#### 516 **Conflicts of interest**

517 The authors declare no conflict of interest.

518

#### 519 **Acknowledgements**

520 This work was supported by grants from the National Natural Science Foundation of China (No. 81573143, 81872612). We thank Dr Hailiang Zhang (Sun Yat-Sen University Cancer Center) for  
 521 81573143, 81872612). We thank Dr Hailiang Zhang (Sun Yat-Sen University Cancer Center) for  
 522 providing Anoxomat Mark III instrument, and thanks to Mr Jim Bacon for critical reading of this  
 523 manuscript. We apologize to the many researchers whose work was not cited in this article due to space  
 524 limitations.

525

## 526 References

- 527 1 M. Potente, H. Gerhardt and P. Carmeliet, Basic and therapeutic aspects of angiogenesis, *Cell*,  
 528 2011, **146**, 873-887.
- 529 2 P. Carmeliet and R. K. Jain, Molecular mechanisms and clinical applications of angiogenesis,  
 530 *Nature*, 2011, **473**, 298-307.
- 531 3 J. Lahteenhuo and A. Rosenzweig, Effects of aging on angiogenesis, *Circ. Res.*, 2012, **110**, 1252-  
 532 1264.
- 533 4 Z. Ungvari, S. Tarantini, T. Kiss, J. D. Wren, C. B. Giles, C. T. Griffin, W. L. Murfee, P. Pacher  
 534 and A. Csizsar, Endothelial dysfunction and angiogenesis impairment in the ageing vasculature,  
 535 *Nat. Rev. Cardiol.*, 2018, **15**, 555-565.
- 536 5 L. Morbidelli, E. Terzuoli and S. Donnini, Use of Nutraceuticals in Angiogenesis-Dependent  
 537 Disorders, *Molecules*, 2018, **23**, 2676.
- 538 6 N. Mazarakis, K. Snibson, P. V. Licciardi and T. C. Karagiannis, The potential use of l-  
 539 sulforaphane for the treatment of chronic inflammatory diseases: A review of the clinical  
 540 evidence, *Clin. Nutr.*, 2020, **39**, 664-675.
- 541 7 A. Briones-Herrera, D. Eugenio-Perez, J. G. Reyes-Ocampo, S. Rivera-Mancia and J. Pedraza-  
 542 Chaverri, New highlights on the health-improving effects of sulforaphane, *Food Funct.*, 2018, **9**,  
 543 2589-2606.
- 544 8 S. Zhang, J. Zhao, Z. Bai, L. Luo, F. Wu, B. Li and Y. Shan, Sulforaphane inhibits the production  
 545 of A $\beta$  partially through the activation of Nrf2-regulated oxidative stress, *Food Funct.*, 2021, **12**,  
 546 11482-11490.
- 547 9 Y. Yagishita, J. W. Fahey, A. T. Dinkova-Kostova and T. W. Kensler, Broccoli or Sulforaphane:  
 548 Is It the Source or Dose That Matters? *Molecules*, 2019, **24**, 3593.
- 549 10 M. Russo, C. Spagnuolo, G. L. Russo, K. Skalicka-Wozniak, M. Daglia, E. Sobarzo-Sanchez, S.  
 550 F. Nabavi and S. M. Nabavi, Nrf2 targeting by sulforaphane: A potential therapy for cancer  
 551 treatment, *Crit. Rev. Food Sci. Nutr.*, 2018, **58**, 1391-1405.
- 552 11 M. Asakage, N. H. Tsuno, J. Kitayama, T. Tsuchiya, S. Yoneyama, J. Yamada, Y. Okaji, S.

- 553 Kaisaki, T. Osada, K. Takahashi and H. Nagawa, Sulforaphane induces inhibition of human  
554 umbilical vein endothelial cells proliferation by apoptosis, *Angiogenesis*, 2006, **9**, 83-91.
- 555 12 T. Nishikawa, N. H. Tsuno, Y. Okaji, E. Sunami, Y. Shuno, K. Sasaki, K. Hongo, M. Kaneko, M.  
556 Hiyoshi, K. Kawai, J. Kitayama, K. Takahashi and H. Nagawa, The inhibition of autophagy  
557 potentiates anti-angiogenic effects of sulforaphane by inducing apoptosis, *Angiogenesis*, 2010, **13**,  
558 227-238.
- 559 13 E. Bertl, H. Bartsch and C. Gerhauser, Inhibition of angiogenesis and endothelial cell functions  
560 are novel sulforaphane-mediated mechanisms in chemoprevention, *Mol. Cancer Ther.*, 2006, **5**,  
561 575-585.
- 562 14 B. Annabi, S. Rojas-Sutterlin, M. Laroche, M. P. Lachambre, R. Moumdjian and R. Beliveau, The  
563 diet-derived sulforaphane inhibits matrix metalloproteinase-9-activated human brain  
564 microvascular endothelial cell migration and tubulogenesis, *Mol. Nutr. Food Res.*, 2008, **52**, 692-  
565 700.
- 566 15 B. Gupta, L. Chiang, K. Chae and D. H. Lee, Phenethyl isothiocyanate inhibits hypoxia-induced  
567 accumulation of HIF-1 $\alpha$  and VEGF expression in human glioma cells, *Food Chem.*, 2013,  
568 **141**, 1841-1846.
- 569 16 D. H. Kim, B. Sung, Y. J. Kang, S. Y. Hwang, M. J. Kim, J.-H. Yoon, E. Im and N. D. Kim,  
570 Sulforaphane inhibits hypoxia-induced HIF-1 $\alpha$  and VEGF expression and migration of human  
571 colon cancer cells, *Int. J. Oncol.*, 2015, **47**, 2226-2232.
- 572 17 Y. Wang, Z. Zhou, W. Wang, M. Liu and Y. Bao, Differential effects of sulforaphane in  
573 regulation of angiogenesis in a co-culture model of endothelial cells and pericytes, *Oncol. Rep.*,  
574 2017, **37**, 2905-2912.
- 575 18 D. Xiao and S. V. Singh, Phenethyl isothiocyanate inhibits angiogenesis in vitro and ex vivo,  
576 *Cancer Res.*, 2007, **67**, 2239-2246.
- 577 19 S. J. Jackson, K. W. Singletary and R. C. Venema, Sulforaphane suppresses angiogenesis and  
578 disrupts endothelial mitotic progression and microtubule polymerization, *Vasc. Pharmacol.*, 2007,  
579 **46**, 77-84.
- 580 20 P. Thejass and G. Kuttan, Allyl isothiocyanate (AITC) and phenyl isothiocyanate (PITC) inhibit  
581 tumour-specific angiogenesis by downregulating nitric oxide (NO) and tumour necrosis factor-  
582 alpha (TNF-alpha) production, *Nitric Oxide*, 2007, **16**, 247-257.
- 583 21 R. Davis, K. P. Singh, R. Kurzrock and S. Shankar, Sulforaphane inhibits angiogenesis through  
584 activation of FOXO transcription factors, *Oncol. Rep.*, 2009, **22**, 1473-1478.
- 585 22 P. Liu, S. J. Atkinson, S. E. Akbareian, Z. Zhou, A. Munsterberg, S. D. Robinson and Y. Bao,  
586 Sulforaphane exerts anti-angiogenesis effects against hepatocellular carcinoma through inhibition  
587 of STAT3/HIF-1 $\alpha$ /VEGF signalling, *Sci. Rep.*, 2017, **7**, 12651.

- 588 23 S. R. Boreddy, R. P. Sahu and S. K. Srivastava, Benzyl isothiocyanate suppresses pancreatic  
 589 tumor angiogenesis and invasion by inhibiting HIF- $\alpha$ /VEGF/Rho-GTPases: pivotal role of  
 590 STAT-3, *PLoS One*, 2011, **6**, e25799.
- 591 24 P. Liu, M. Behray, Q. Wang, W. Wang, Z. Zhou, Y. Chao and Y. Bao, Anti-cancer activities of  
 592 allyl isothiocyanate and its conjugated silicon quantum dots, *Sci. Rep.*, 2018, **8**, 1804.
- 593 25 P. Sestili and C. Fimognari, Cytotoxic and Antitumor Activity of Sulforaphane: The Role of  
 594 Reactive Oxygen Species, *Biomed Res. Int.*, 2015, **2015**, 402386.
- 595 26 S. Pal and V. B. Konkimalla, Hormetic Potential of Sulforaphane (SFN) in Switching Cells' Fate  
 596 Towards Survival or Death, *Mini-Rev. Med. Chem.*, 2016, **16**, 980-995.
- 597 27 K. M. Holmstrom, R. V. Kostov and A. T. Dinkova-Kostova, The multifaceted role of Nrf2 in  
 598 mitochondrial function, *Current opinion in toxicology*, 2016, **1**, 80-91.
- 599 28 Y. Wei, J. Gong, R. K. Thimmulappa, B. Kosmider, S. Biswal and E. J. Duh, Nrf2 acts cell-  
 600 autonomously in endothelium to regulate tip cell formation and vascular branching, *Proc. Natl.*  
 601 *Acad. Sci. U. S. A.*, 2013, **110**, e3910-e3918.
- 602 29 X. Dai, X. Yan, J. Zeng, J. Chen, Y. Wang, J. Chen, Y. Li, M. T. Barati, K. A. Wintergerst, K.  
 603 Pan, M. A. Nystoriak, D. J. Conklin, G. Rokosh, P. N. Epstein, X. Li and Y. Tan, Elevating  
 604 CXCR7 Improves Angiogenic Function of EPCs via Akt/GSK-3 $\beta$ /Fyn-Mediated Nrf2 Activation  
 605 in Diabetic Limb Ischemia, *Circ. Res.*, 2017, **120**, e7-e23.
- 606 30 H. K. Na and Y. J. Surh, Oncogenic potential of Nrf2 and its principal target protein heme  
 607 oxygenase-1, *Free Radic Biol. Med.*, 2014, **67**, 353-365.
- 608 31 Z. Guo and Z. Mo, Keap1-Nrf2 signaling pathway in angiogenesis and vascular diseases, *J. Tissue*  
 609 *Eng. Regen. Med.*, 2020, **14**, 869-883.
- 610 32 R. Marcu, Y. Zheng and B. J. Hawkins, Mitochondria and Angiogenesis, *Adv. Exp. Med. Biol.*,  
 611 2017, **982**, 371-406.
- 612 33 J. J. Lugus, G. A. Ngoh, M. M. Bachschmid and K. Walsh, Mitofusins are required for angiogenic  
 613 function and modulate different signaling pathways in cultured endothelial cells, *J. Mol. Cell*  
 614 *Cardiol.*, 2011, **51**, 885-893.
- 615 34 S. L. Archer, Mitochondrial dynamics--mitochondrial fission and fusion in human diseases, *N.*  
 616 *Engl. J. Med.*, 2013, **369**, 2236-2251.
- 617 35 V. Eisner, M. Picard and G. Hajnóczky, Mitochondrial dynamics in adaptive and maladaptive  
 618 cellular stress responses, *Nat. Cell Biol.*, 2018, **20**, 755-765.
- 619 36 H. G. Sprenger and T. Langer, The Good and the Bad of Mitochondrial Breakups, *Trends Cell*  
 620 *Biol.*, 2019, **29**, 888-900.
- 621 37 H. Zhou, S. Wang, P. Zhu, S. Hu, Y. Chen and J. Ren, Empagliflozin rescues diabetic myocardial



- 622 microvascular injury via AMPK-mediated inhibition of mitochondrial fission, *Redox Biol.* **2018**, View Article Online  
DOI: 10.1016/j.redox.2018.10.039/D1FO04112F  
623 **15**, 335-346.
- 624 38 L. Hu, M. Ding, D. Tang, E. Gao, C. Li, K. Wang, B. Qi, J. Qiu, H. Zhao, P. Chang, F. Fu and Y.  
625 Li, Targeting mitochondrial dynamics by regulating Mfn2 for therapeutic intervention in diabetic  
626 cardiomyopathy, *Theranostics*, 2019, **9**, 3687-3706.
- 627 39 B. B. Yu, H. Zhi, X. Y. Zhang, J. W. Liang, J. He, C. Su, W. H. Xia, G. X. Zhang and J. Tao,  
628 Mitochondrial dysfunction-mediated decline in angiogenic capacity of endothelial progenitor cells  
629 is associated with capillary rarefaction in patients with hypertension via downregulation of  
630 CXCR4/JAK2/SIRT5 signaling, *EBioMedicine*, 2019, **42**, 64-75.
- 631 40 A. Sehwat, R. Roy, S. K. Pore, E. R. Hahm, S. K. Samanta, K. B. Singh, S. H. Kim, K. Singh  
632 and S. V. Singh, Mitochondrial dysfunction in cancer chemoprevention by phytochemicals from  
633 dietary and medicinal plants, *Semin. Cancer Biol.*, 2017, **47**, 147-153.
- 634 41 K. H. Tsui, M. Y. Wu, L. T. Lin, Z. H. Wen, Y. H. Li, P. Y. Chu and C. J. Li, Disruption of  
635 mitochondrial homeostasis with artemisinin unravels anti-angiogenesis effects via auto-paracrine  
636 mechanisms, *Theranostics*, 2019, **9**, 6631-6645.
- 637 42 S. T. Huang, C. C. Huang, J. M. Sheen, T. K. Lin, P. L. Liao, W. L. Huang, P. W. Wang, C. W.  
638 Liou and J. H. Chuang, Phyllanthus urinaria's Inhibition of Human Osteosarcoma Xenografts  
639 Growth in Mice is Associated with Modulation of Mitochondrial Fission/Fusion Machinery, *Am.  
640 J. Chin. Med.*, 2016, **44**, 1507-1523.
- 641 43 M. Negrette-Guzman, S. Huerta-Yepez, E. Tapia and J. Pedraza-Chaverri, Modulation of  
642 mitochondrial functions by the indirect antioxidant sulforaphane: a seemingly contradictory dual  
643 role and an integrative hypothesis, *Free Radic Biol. Med.*, 2013, **65**, 1078-1089.
- 644 44 M. Negrette-Guzmán, S. Huerta-Yepez, M. I. Vega, J. C. León-Contreras, R. Hernández-Pando,  
645 O. N. Medina-Campos, E. Rodríguez, E. Tapia and J. Pedraza-Chaverri, Sulforaphane induces  
646 differential modulation of mitochondrial biogenesis and dynamics in normal cells and tumor cells,  
647 *Food Chem. Toxicol.*, 2017, **100**, 90-102.
- 648 45 Y. Geng, Y. Zhou, S. Wu, Y. Hu, K. Lin, Y. Wang, Z. Zheng and W. Wu, Sulforaphane Induced  
649 Apoptosis via Promotion of Mitochondrial Fusion and ERK1/2-Mediated 26S Proteasome  
650 Degradation of Novel Pro-survival Bim and Upregulation of Bax in Human Non-Small Cell Lung  
651 Cancer Cells, *J. Cancer*, 2017, **8**, 2456-2470.
- 652 46 G. B. O'Mealey, W. L. Berry and S. M. Plafker, Sulforaphane is a Nrf2-independent inhibitor of  
653 mitochondrial fission, *Redox Biol.*, 2017, **11**, 103-110.
- 654 47 I. C. Lavich, B. S. de Freitas, L. W. Kist, L. Falavigna, V. A. Dargel, L. M. Kobe, C. Aguzzoli, B.  
655 Piffero, P. Z. Florian, M. R. Bogo, M. N. de Lima and N. Schroder, Sulforaphane rescues memory  
656 dysfunction and synaptic and mitochondrial alterations induced by brain iron accumulation,  
657 *Neuroscience*, 2015, **301**, 542-552.

- 658 48 A. Sehwat, C. S. Croix, C. J. Baty, S. Watkins, D. Taylor, R. P. Singh and S. V. Singh, DOI: 10.1039/D1FO04112F  
659 Inhibition of mitochondrial fusion is an early and critical event in breast cancer cell apoptosis by  
660 dietary chemopreventative benzyl isothiocyanate, *Mitochondrion*, 2016, **30**, 67-77.
- 661 49 G. B. Li, J. Zhou, A. Budhraj, X. Y. Hu, Y. B. Chen, Q. Cheng, L. Liu, T. Zhou, P. Li, E. H. Liu  
662 and N. Gao, Mitochondrial translocation and interaction of cofilin and Drp1 are required for  
663 erucin-induced mitochondrial fission and apoptosis, *Oncotarget*, 2015, **6**, 1834-1849.
- 664 50 P. H. G. M. Willems, R. Rossignol, C. E. J. Dieteren, M. P. Murphy and W. J. H. Koopman,  
665 Redox Homeostasis and Mitochondrial Dynamics, *Cell Metab.*, 2015, **22**, 207-218.
- 666 51 Y. M. Kim, S. W. Youn, V. Sudhakar, A. Das, R. Chandhri, H. Cuervo Grajal, J. Kweon, S.  
667 Leanhart, L. He, P. T. Toth, J. Kitajewski, J. Rehman, Y. Yoon, J. Cho, T. Fukai and M. Ushio-  
668 Fukai, Redox Regulation of Mitochondrial Fission Protein Drp1 by Protein Disulfide Isomerase  
669 Limits Endothelial Senescence, *Cell Rep.*, 2018, **23**, 3565-3578.
- 670 52 M. P. Mattson, Dietary factors, hormesis and health, *Ageing Res. Rev.*, 2008, **7**, 43-48.
- 671 53 A. M. Walters, G. A. Porter and P. S. Brookes, Mitochondria as a Drug Target in Ischemic Heart  
672 Disease and Cardiomyopathy, *Circ. Res.*, 2012, **111**, 1222-1236.
- 673 54 C. Befani and P. Liakos, Hypoxia upregulates integrin gene expression in microvascular  
674 endothelial cells and promotes their migration and capillary-like tube formation, *Cell Biol. Int.*,  
675 2017, **41**, 769-778.
- 676 55 Y. C. Lee, Y. C. Chang, C. C. Wu and C. C. Huang, Hypoxia-Preconditioned Human Umbilical  
677 Vein Endothelial Cells Protect Against Neurovascular Damage After Hypoxic Ischemia in  
678 Neonatal Brain, *Mol. Neurobiol.*, 2018, **55**, 7743-7757.
- 679 56 S. Schwalm, F. Doll, I. Romer, S. Bubnova, J. Pfeilschifter and A. Huwiler, Sphingosine kinase-1  
680 is a hypoxia-regulated gene that stimulates migration of human endothelial cells, *Biochem.*  
681 *Biophys. Res. Commun.*, 2008, **368**, 1020-1025.
- 682 57 D. J. Manalo, A. Rowan, T. Lavoie, L. Natarajan, B. D. Kelly, S. Q. Ye, J. G. Garcia and G. L.  
683 Semenza, Transcriptional regulation of vascular endothelial cell responses to hypoxia by HIF-1,  
684 *Blood*, 2005, **105**, 659-669.
- 685 58 W. Li, M. Petrimpol, K. D. Molle, M. N. Hall, E. J. Battagay and R. Humar, Hypoxia-induced  
686 endothelial proliferation requires both mTORC1 and mTORC2, *Circ. Res.*, 2007, **100**, 79-87.
- 687 59 L. Wang, A. Bhatta, H. A. Toque, M. Rojas, L. Yao, Z. Xu, C. Patel, R. B. Caldwell and R. W.  
688 Caldwell, Arginase inhibition enhances angiogenesis in endothelial cells exposed to hypoxia,  
689 *Microvasc. Res.*, 2015, **98**, 1-8.
- 690 60 N. Hashimoto, K. Ikuma, Y. Konno, M. Hirose, H. Tadokoro, H. Hasegawa, Y. Kobayashi and H.  
691 Takano, DPP-4 inhibition protects human umbilical vein endothelial cells from hypoxia-induced  
692 vascular barrier impairment, *J. Pharmacol. Sci.*, 2017, **135**, 29-36.

- 693 61 I. Baldea, I. Teacoe, D. E. Olteanu, C. Vaida-Voievod, A. Clichici, A. Sirbu, G. A. Filip and S. Clichici, Effects of different hypoxia degrees on endothelial cell cultures-Time course study,  
694 *Mech. Ageing Dev.*, 2018, **172**, 45-50.  
695
- 696 62 M. E. Hubbi and G. L. Semenza, Regulation of cell proliferation by hypoxia-inducible factors,  
697 *Am. J. Physiol.: Cell Physiol.*, 2015, **309**, C775-C782.
- 698 63 I. Filippi, I. Saltarella, C. Aldinucci, F. Carraro, R. Ria, A. Vacca and A. Naldini, Different  
699 Adaptive Responses to Hypoxia in Normal and Multiple Myeloma Endothelial Cells, *Cell*  
700 *Physiol. Biochem.*, 2018, **46**, 203-212.
- 701 64 Y. P. Bao, W. Wang, Z. G. Zhou and C. H. Sun, Benefits and Risks of the Hormetic Effects of  
702 Dietary Isothiocyanates on Cancer Prevention, *Plos One*, 2014, **9**, e114764.
- 703 65 G. Wang, J. H. Nie, Y. Bao and X. Yang, Sulforaphane Rescues Ethanol-Suppressed  
704 Angiogenesis through Oxidative and Endoplasmic Reticulum Stress in Chick Embryos, *J. Agric.*  
705 *Food Chem.*, 2018, **66**, 9522-9533.
- 706 66 H. Gremmels, O. G. de Jong, D. H. Hazenbrink, J. O. Fledderus and M. C. Verhaar, The  
707 Transcription Factor Nrf2 Protects Angiogenic Capacity of Endothelial Colony-Forming Cells in  
708 High-Oxygen Radical Stress Conditions, *Stem Cells Int.*, 2017, **2017**, 4680612.
- 709 67 U. Florczyk, A. Jazwa, M. Maleszewska, M. Mendel, K. Szade, M. Kozakowska, A. Grochot-  
710 Przekzek, M. Viscardi, S. Czauderna, K. Bukowska-Strakova, J. Kotlinowski, A. Jozkowicz, A.  
711 Loboda and J. Dulak, Nrf2 regulates angiogenesis: effect on endothelial cells, bone marrow-  
712 derived proangiogenic cells and hind limb ischemia, *Antioxid. Redox Signaling*, 2014, **20**, 1693-  
713 1708.
- 714 68 L. H. Kuang, J. Feng, G. X. He and T. Jing, Knockdown of Nrf2 Inhibits the Angiogenesis of Rat  
715 Cardiac Micro-vascular Endothelial Cells under Hypoxic Conditions, *Int. J. Biol. Sci.*, 2013, **9**,  
716 656-665.
- 717 69 R. Sabouny, E. Fraunberger, M. Geoffrion, A. C. Ng, S. D. Baird, R. A. Sreaton, R. Milne, H. M.  
718 McBride and T. E. Shutt, The Keap1-Nrf2 Stress Response Pathway Promotes Mitochondrial  
719 Hyperfusion Through Degradation of the Mitochondrial Fission Protein Drp1, *Antioxid. Redox*  
720 *Signaling*, 2017, **27**, 1447-1459.
- 721 70 Y. Liu, J. W. Yan, C. Sun, G. Li, S. R. Li, L. W. Zhang, C. X. Di, L. Gan, Y. P. Wang, R. Zhou, J.  
722 Si and H. Zhang, Ameliorating mitochondrial dysfunction restores carbon ion-induced cognitive  
723 deficits via co-activation of NRF2 and PINK1 signaling pathway, *Redox Biol.*, 2018, **17**, 143-157.
- 724 71 Y. He, X. Gan, L. Zhang, B. Liu, Z. Zhu, T. Li, J. Zhu, J. Chen and H. Yu, CoCl<sub>2</sub> induces  
725 apoptosis via a ROS-dependent pathway and Drp1-mediated mitochondria fission in periodontal  
726 ligament stem cells, *Am. J. Physiol.: Cell Physiol.*, 2018, **315**, C389-C397.
- 727 72 Q. Han, G. Li, M. S. Ip, Y. Zhang, Z. Zhen, J. C. Mak and N. Zhang, Haemin attenuates  
728 intermittent hypoxia-induced cardiac injury via inhibiting mitochondrial fission, *J. Cell Mol.*

729 *Med.*, 2018, **22**, 2717-2726.

730

### 731 **Figure legends**

732 **Fig. 1. SFN treatment bilaterally affects hypoxia-induced angiogenesis in HUVECs.** HUVECs  
733 were treated with indicated concentrations of SFN under hypoxia with DMSO ( $\leq 1\%$ ) treatment under  
734 normoxia or hypoxia as different controls. **a** HUVECs proliferation was measured by a WST-1 assay at  
735 24h. Data are presented as mean  $\pm$  SD of six independent experiments carried out in sextuplicate.  
736 \* $p < 0.05$ , \*\* $p < 0.01$  vs. normoxia control; # $p < 0.05$ , ## $p < 0.01$  vs. hypoxia control. **b,c** HUVECs  
737 migration was determined by transwell assays at 24h. Representative pictures depicting HUVECs  
738 migration (scale bar = 100  $\mu\text{m}$ ) and quantitative analysis of the migrated cells numbers are presented.  
739 Data represents mean  $\pm$  SD of three independent experiments carried out in triplicate. \* $p < 0.05$ , \*\* $p$   
740  $< 0.01$  vs. normoxia control; # $p < 0.05$ , ## $p < 0.01$  vs. hypoxia control. **d-g** Capillary-like structure  
741 formation by HUVECs was detected at 8h. Representative images of capillary-like structures (scale bar  
742 = 200  $\mu\text{m}$ ) (**d**) and quantification of the number of meshes (**e**) and nodes (**f**) as well as the total lengths  
743 of branches (**g**) are shown. All values are expressed as mean  $\pm$  SD of three independent experiments  
744 carried out in triplicate. \* $p < 0.05$ , \*\* $p < 0.01$  vs. normoxia control; # $p < 0.05$ , ## $p < 0.01$  vs. hypoxia  
745 control.

746

747 **Fig. 2. Nrf2/HO-1-mediated pro-angiogenesis contributes to the angio-modulatory property of**  
748 **SFN in HUVECs under hypoxia.** **a, b** Representative immunoblots and relative densitometric  
749 analysis of Nrf2 and HO-1 in the whole HUVECs exposed to 1.25-20 $\mu\text{M}$  SFN for 24h under hypoxia  
750 with DMSO ( $< 1\%$ ) intervention under normoxia and hypoxia as different controls. The results are  
751 presented as mean  $\pm$  SD of three independent experiments. \* $p < 0.05$ , \*\* $p < 0.01$  vs. normoxia control;  
752 # $p < 0.05$ , ## $p < 0.01$  vs. hypoxia control. HUVECs were transfected with 10nM Nrf2 siRNA or con  
753 siRNA for 8h. The medium was then replaced and incubation continued for 24h under normoxia,  
754 followed by SFN (2.5, 10 $\mu\text{M}$ ) or DMSO ( $< 1\%$ ) intervention under hypoxia. **c, d** The protein levels of  
755 Nrf2 and HO-1 were detected by Western blots analysis after 24h intervention. The results are  
756 presented as mean  $\pm$  SD of three independent experiments. \* $p < 0.05$ , \*\* $p < 0.01$  vs. DMSO-treated

757 siCON; # $p$ <0.05, ## $p$ <0.01 between equivalent SFN or DMSO-treated siNrf2 and siCON. **e-h** Tube  
758 formation was determined by *in vitro* Matrigel angiogenesis assay after 8h treatment. Representative  
759 images of capillary-like structures (scale bar = 200  $\mu$ m) (**e**) and quantification of the number of meshes  
760 (**f**) and nodes (**g**) as well as the total lengths of branches (**h**) are shown. All values are expressed as  
761 mean  $\pm$  SD of three independent experiments carried out in triplicate. \* $p$ <0.05, \*\* $p$ <0.01 vs. DMSO-  
762 treated siCON; ## $p$ <0.01 between equivalent SFN or DMSO-treated siNrf2 and siCON.

763

764 **Fig. 3. SFN treatment bilaterally affects hypoxia-induced mitochondrial injury and fission in**  
765 **HUVECs.** HUVECs were exposed to the indicated concentration of SFN under hypoxia for 24h with  
766 DMSO (<1%) intervention under normoxia and hypoxia as different controls. **a, b** Representative  
767 ultrastructure of mitochondria by transmission electron microscopy (magnification $\times$ 30,000; scale bar =  
768 500 nm) and percentage of mitochondrial injuries in each condition. For quantification, at least 300  
769 mitochondria per condition were analyzed. Mitochondrial injuries were categorized into entirely  
770 damaged and partially damaged phenotypes, and the former was scored in the absence of cristae and  
771 the latter scored if some cristae were present, compared to intact mitochondria with normal cristae. **c**  
772 Quantification of the mitochondrial membrane potential ( $mt\Delta\Psi$ ) was done using fluorescence probe  
773 JC-1 and a microplate reader with  $mt\Delta\Psi$  values calculated as the ratio of red/green fluorescence  
774 intensity. Data are presented as mean  $\pm$  SD of three independent experiments carried out in  
775 quintuplicate. \* $p$ <0.05, \*\* $p$ <0.01 vs. normoxia control; # $p$ <0.05, ## $p$ <0.01 vs. hypoxia control. **d**  
776 Representative morphology of mitochondria by confocal microscopy after staining with mitochondrial  
777 fluorescent dye MitoTracker Green (panels on the left: scale bar = 25  $\mu$ m; middle: scale bar =15 $\mu$ m). **e,**  
778 **f** Quantification of mitochondrial circularity and lengths in the fluorescence photograph by computer-  
779 assisted morphometric analysis. Data are presented as mean  $\pm$  SD of three independent experiments  
780 carried out in triplicate and at least 60 cells per group were analyzed. \* $p$ <0.05, \*\* $p$ <0.01 vs. normoxia  
781 control; # $p$ <0.05, ## $p$ <0.01 vs. hypoxia control.

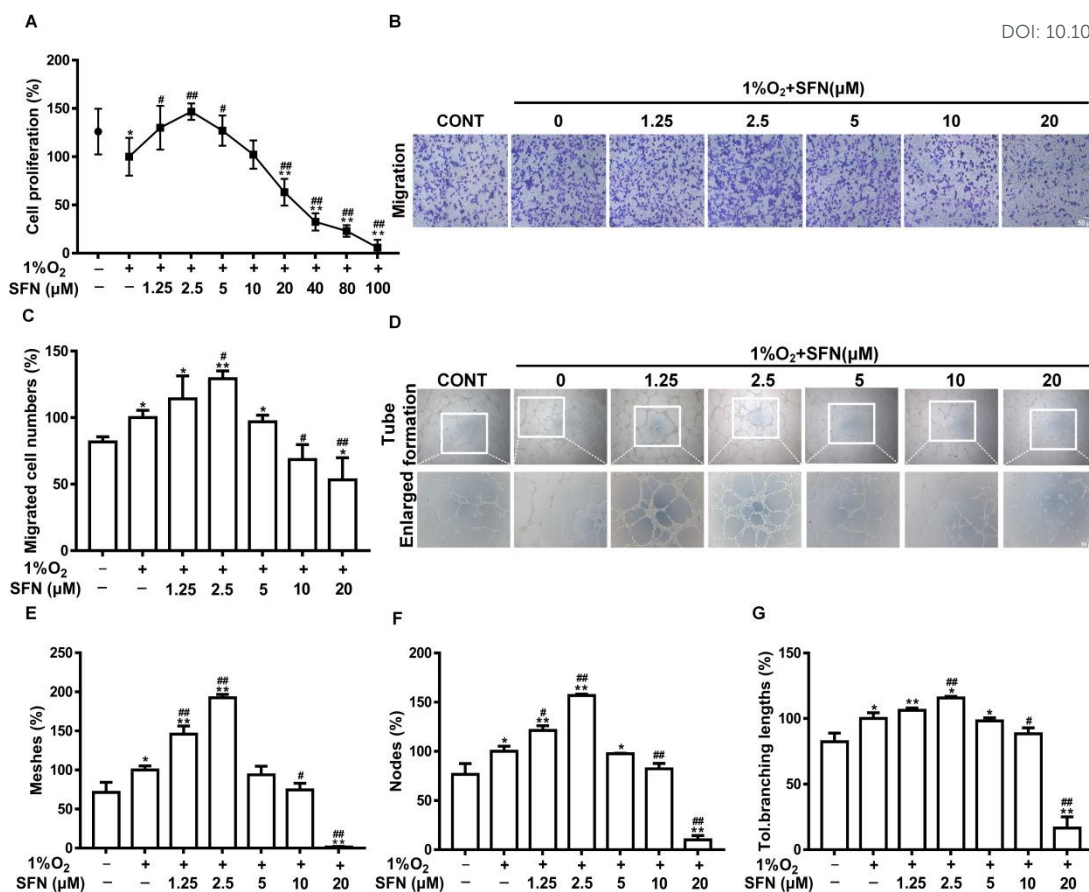
782

783 **Fig. 4. Effect of SFN on hypoxia-induced alteration in dynamics related protein levels in**  
784 **HUVECs.** HUVECs were exposed to normoxia or hypoxia treatment alone or hypoxia in

785 combination with SFN (1.25-20 $\mu$ M) treatment, respectively, for 24h. Representative Western blots  
786 images and bands densitometric quantification showing the levels of the pro-fission proteins Drp1 (**a**)  
787 and Fis1 (**b**), the pro-fusion proteins Mfn1/2 (**c, d**) and Opa1(**e**), with  $\beta$ -actin as loading control. Data  
788 are presented as mean  $\pm$  SD of three independent experiments. \* $p$ <0.05, \*\* $p$  <0.01 vs. normoxia  
789 control; # $p$ <0.05, ## $p$  <0.01 vs. hypoxia control.

790

791 **Fig. 5. Effect of SFN on mitochondrial morphology after Nrf2 knockdown in HUVECs under**  
792 **hypoxia.** HUVECs were transfected with 10nM nrf2 siRNA or con siRNA for 8h. The medium was  
793 then replaced and incubation continued for 24h under normoxia, followed by SFN (2.5, 10 $\mu$ M) or  
794 DMSO (<1%) treatment for 24h under hypoxia. Mitochondria morphology was detected by  
795 MitoTracker Green staining. **a** Representative fluorescence images captured by confocal microscopy  
796 (panels on the left: scale bar = 25  $\mu$ m; middle: scale bar =15 $\mu$ m). **b, c** Statistical data of the quantified  
797 mitochondrial circularity and lengths were shown as histograms. Data are means  $\pm$  SD of triplicate  
798 determinations and at least 30 cells per group were analyzed. \* $p$ <0.05, \*\* $p$  <0.01 vs. DMSO-treated  
799 siCON; # $p$ <0.05, ## $p$  <0.01 between equivalent SFN or DMSO-treated siNrf2 and siCON.



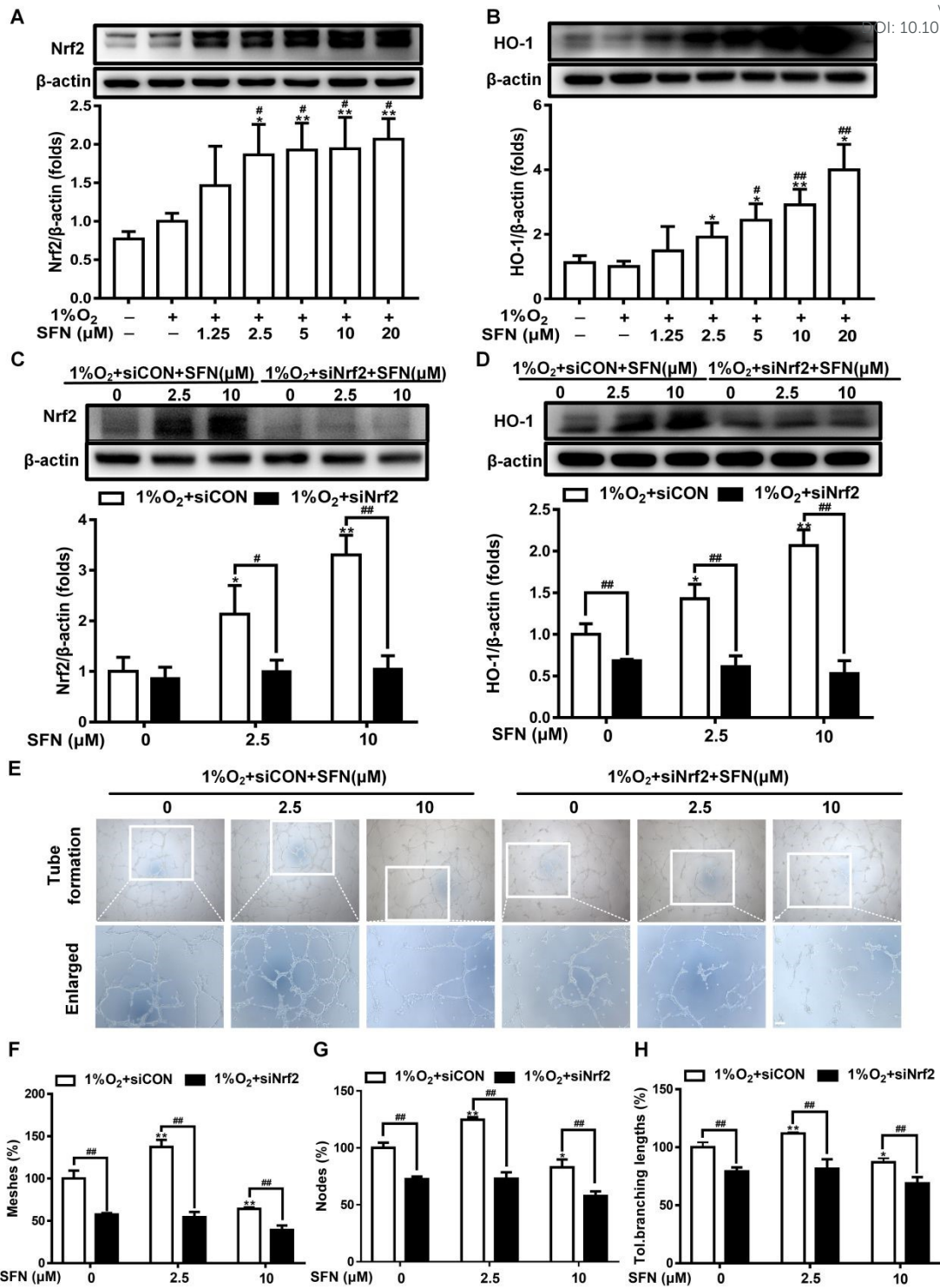
800

801

**Fig. 1. SFN treatment bilaterally affects hypoxia-induced angiogenesis in HUVECs.**

802

803

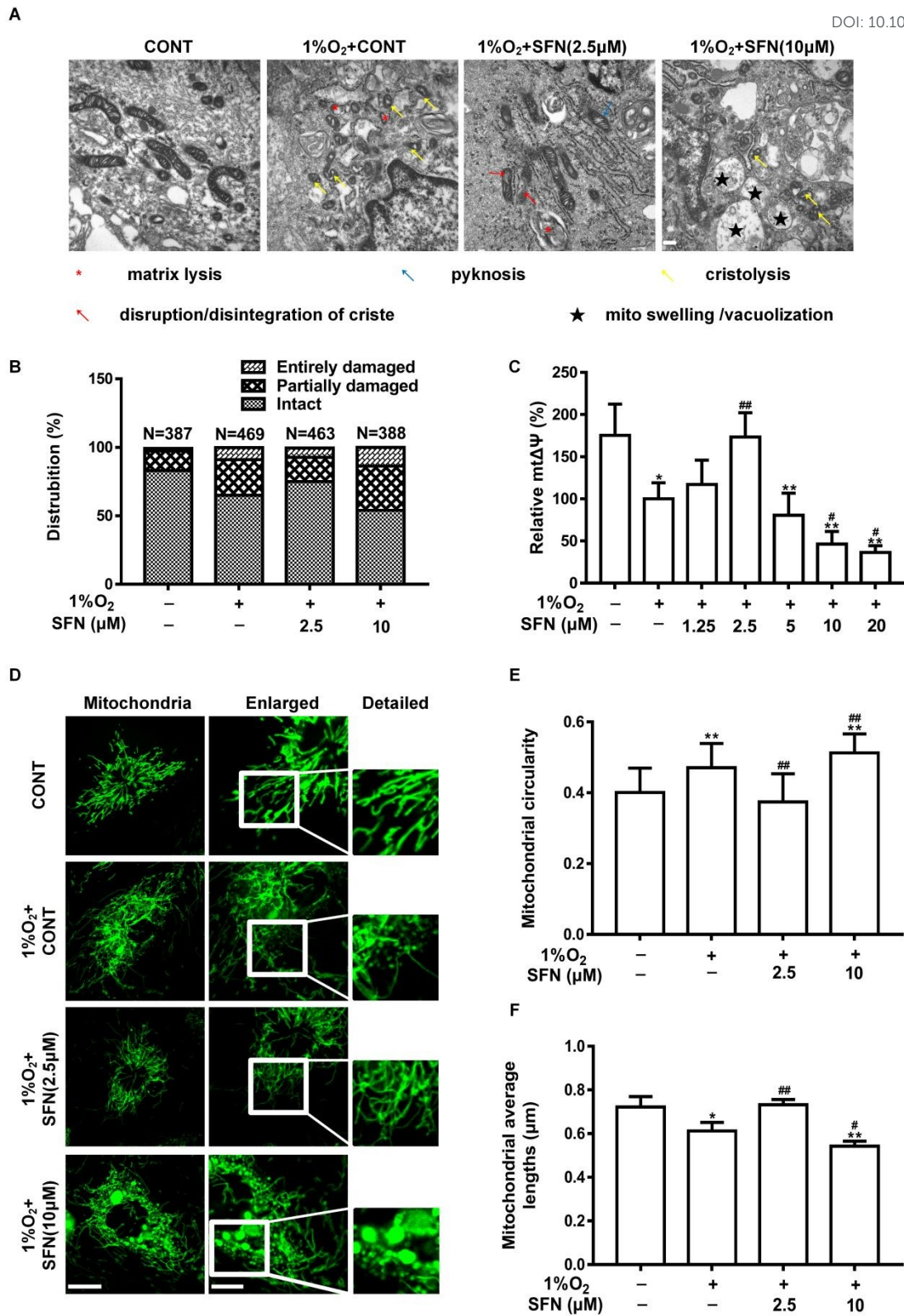


804

805 Fig. 2. Nrf2/HO-1-mediated pro-angiogenesis contributes to the angio-modulatory property of

806 SFN in HUVECs under hypoxia.



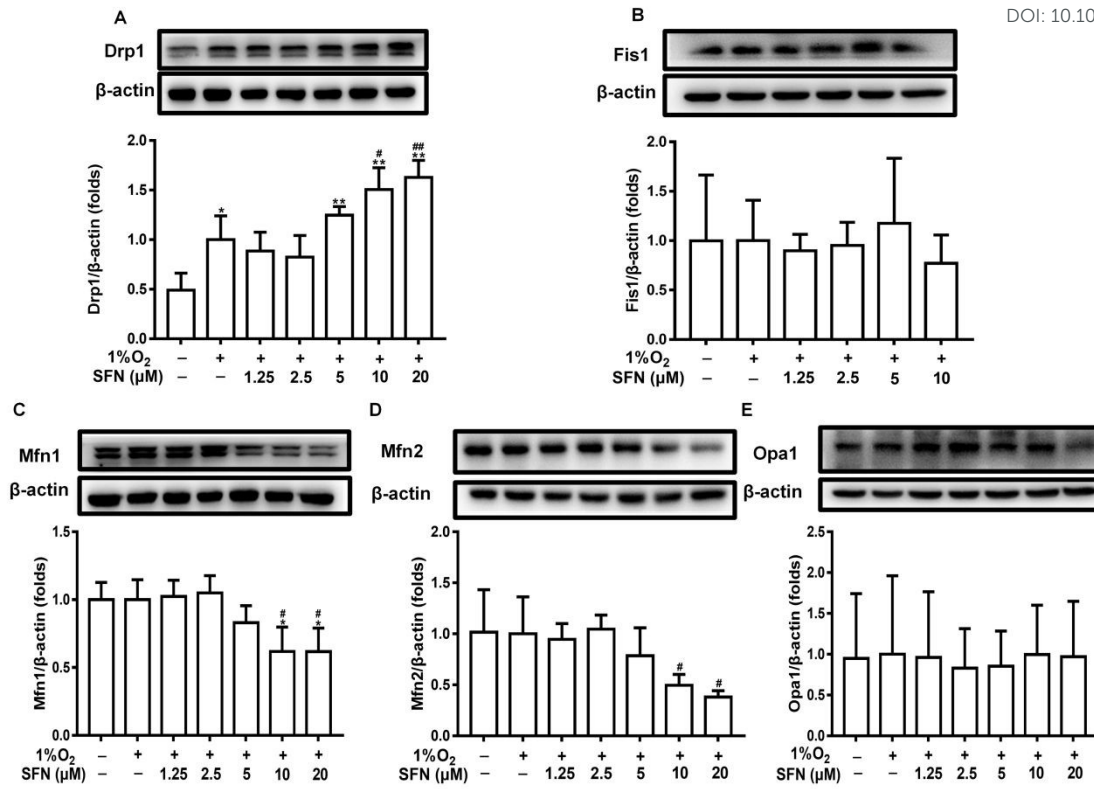


Food & Function Accepted Manuscript

807

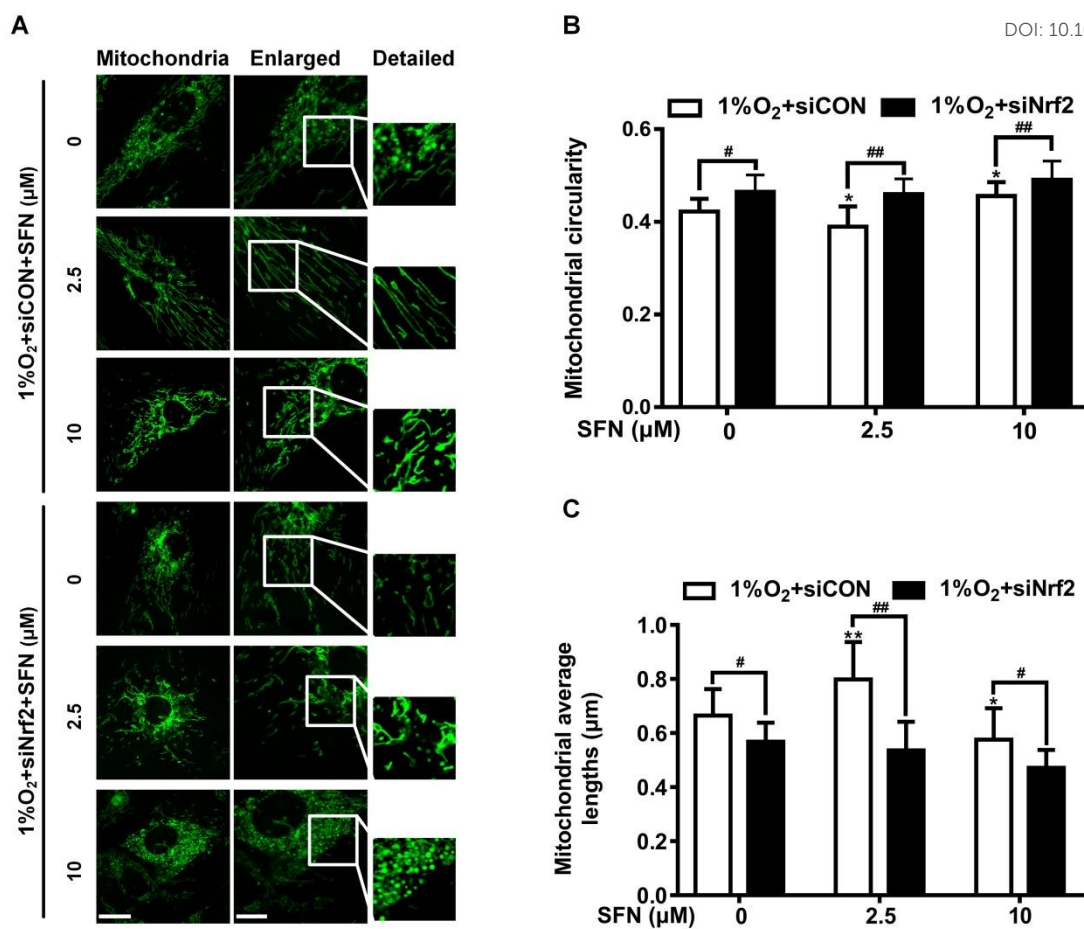
808 **Fig. 3.** SFN treatment bilaterally affects hypoxia-induced mitochondrial injury and fission in  
809 HUVECs.

Published on 14 February 2022. Downloaded by Sun Yat-Sen (Zhongshan) University on 2/14/2022 10:46:14 AM.



810

811 **Fig. 4. Effect of SFN on hypoxia-induced alteration in dynamics related proteins levels in**812 **HUVECs.**



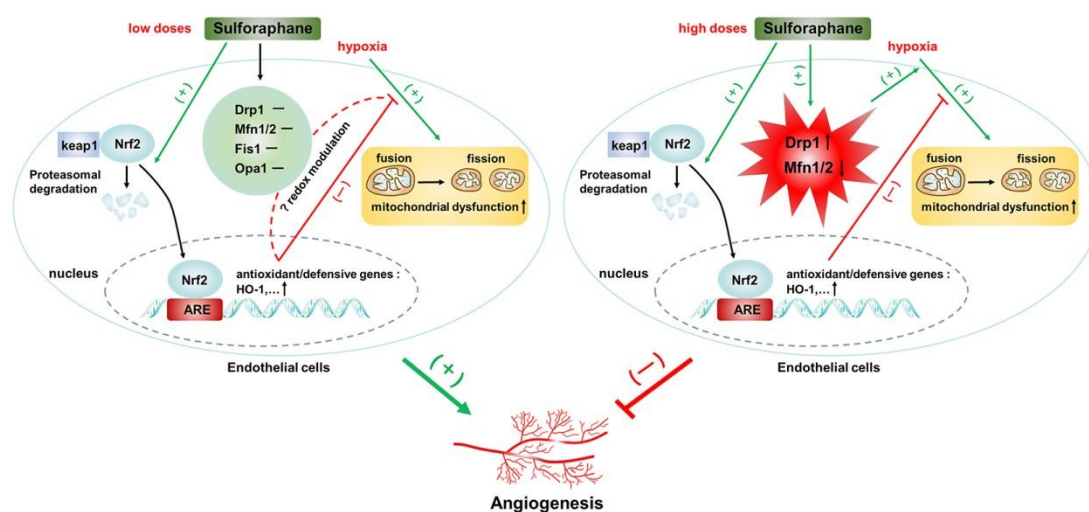
813

814 **Fig. 5. Effect of SFN on mitochondrial morphology after Nrf2 knockdown in HUVECs under**  
 815 **hypoxia.**

816

817

818



819

820 **Fig. 6. Proposed mechanism of biphasic effect of SFN on angiogenesis in hypoxia.**

821 The angio-hormetic effect of SFN in hypoxia may be mainly ascribed to its mito-hormetic effect via an  
 822 integrated modulation of Nrf2 and mitochondrial dynamics. Nrf2 activation by moderate doses of SFN  
 823 contributes to the protection against hypoxia-evoked mitochondrial injury and fission thus boosting  
 824 the angiogenic capacity of vascular endothelial cells. However, under high dose of SFN exposure, the  
 825 induction of mitochondrial fission resulting from up-regulating Drp1 and down-regulating Mfn1/2,  
 826 coupled with aggravated mitochondrial injury, overwhelms Nrf2-mediated defense, hence generating  
 827 an angio-inhibitory effect.

828